Perfluoroalkyl End-Capped Poly(ethylene oxide). Synthesis, Characterization, and Rheological Behavior in Aqueous Solution

Damien Calvet, André Collet, and Michel Viguier*

Laboratoire "Organisation Moléculaire. Evolution et Matériaux fluorés", UMR CNRS / Université Montpellier II No. 5073, F-34095 Montpellier Cedex 05, France

Jean-François Berret

Complex Fluids Laboratory, CNRS−Cranbury Research Center Rhodia Inc., 259 Prospect Plains Road, Cranbury, New Jersey 08512

Yaelle Séréro

FOM-Institute for Atomic and Molecular Physics, Kruislaan 407, 1098 SJ Amsterdam, The Netherlands

Received October 3, 2001; Revised Manuscript Received October 25, 2002

ABSTRACT: A series of perfluoroalkyl end-capped poly(ethylene oxide) (PEO) of molecular weight M_n = 10 000 and 20 000, noted F-HEUR-10K and F-HEUR-20K, with a well-defined structure were synthesized in two reaction steps. The reaction of PEO with a large excess of isophorone diisocyanate (IPDI) leads to an isocyanate-terminated prepolymer which is then reacted with the semifluorinated alcohol [$C_8F_{17}(CH_2)_{11}$-OH]. Experimental conditions were improved to prevent polycondensation in the first step of the synthesis. The degree of functionalization is controlled by ^{19}F NMR. The influence of the terminal perfluorinated group on the linear viscoelasticity of aqueous solutions has been investigated as a function of the polymer concentration C_{pol}, PEO chain length, degree of functionalization, surfactant (SDS), and temperature. A steep increase of the static viscosity η_0, attributed to the sol−viscoelastic transition with the formation of a multiconnected network, is observed at $C_{pol} \approx 1$ wt %. The stress relaxation function $G(t)$ is best fitted by a stretched exponential $G(t) = G_0 \exp[-(t/\tau)^{\alpha}]$, where G_0 is the elastic plateau modulus. The relaxation time τ and static viscosity η_0 were found to be temperature-dependent according to the Arrhenius law. The hydrophobic character of the end caps reinforced by the perfluorinated segments leads to larger relaxation times (several hundred seconds) and higher activation energies (≈120 kJ mol^{-1}) compared to those of hydrocarbon HEUR-type associative polymers.

1. Introduction

Water-soluble associative polymers (APs) have found important applications as rheology modifiers.[1,2] Pendent hydrophobic groups incorporated into the polymer backbone give rise to intra- and intermolecular associations. In aqueous solutions APs develop viscosifying properties resulting from the formation of a transient network. As a result, these polymers are also called associative thickeners (ATs).

The challenge is to understand the origin of these properties in terms of macromolecular architecture and chemical structure of hydrophobic end groups. In this regard, linear hydrophilic polymers such poly(ethylene oxide) (PEO) end-capped by hydrophobic segments present a rather well-defined architecture by comparison with hydrophobically modified hydroxyethyl celluloses[3,4] or acrylamide polymers.[5] The latter polymers present a random distribution of hydrophobic groups along the polymer chain.

Hydrophobically modified PEO can be obtained by different methods including various linkers used to connect the PEO chain with the hydrophobic segment. The syntheses of modified PEO with linkers such as ethers,[6] esters,[7,8] urethanes,[9,10] or diurethanes[11,12] were reported. It was clearly established that initial aggregation and clouding behavior are very sensitive to subtle changes in the chemical structure of the linker.[10]

Hydrophobically modified ethoxylated urethanes (HEUR) with diurethane junction have attracted interest due to the more staightforward synthesis and a larger versatility. Some of the results reported in the literature refer to HEURs synthesized by step growth polymerization.[13,14] The broad molecular weight distribution of these polymers and the presence of internal alkyl groups increase the complexity of these systems and influence the rheological responses.[15] Various species with distinct molecular weights lead to an imperfect network where lower and higher molecular weights species may be involved preferentially in different types of associations.

To synthesize model hydrophobic telechelic PEOs, one must prevent the polycondensation during the first step of the synthesis leading to isocyanate end-capped PEO. Particular attention is paid in this paper to the synthesis of HEUR with a well-defined overall architecture and especially with a complete chain end functionalization.

Recently, it was shown that PEO end-functionalized with semifluorinated groups [$C_nF_{2n+1}-(CH_2)_m$] called F-HEUR presents stronger hydrophobic association and a higher viscosifying effect than the corresponding hydrocarbon derivatives.[16−19] Small changes in the perfluorinated segment or hydrocarbon spacer $(CH_2)_m$ have a considerable influence on the viscoelasticity.[17,18]

F-HEUR with a narrow molecular weight distribution (determined by size exclusion chromatography) was obtained by using a large excess of isophorone diisocyanate in the first step of the reaction. In this way the presence of PEOs with twice or higher molecular

10.1021/ma011729a CCC: $25.00
Published on Web 12/20/2002

weights is avoided. Polycondensation occurring in the first reaction step could enhance the F-HEUR solubility in water.[18] In nonfluorinated series, HEURs with a broader molecular weight distribution exhibit significantly lower viscosities in aqueous solution at equal concentrations.[15]

Complete end-capping of PEOs is dependent on reaction conditions. In this study, the synthetic procedure was optimized for PEO 20K in order to obtain complete functionalization. The titration of residual OH groups is performed by reaction with trifluoroacetic anhydride and ^{19}F NMR analysis. In this way it is possible to get an indication about the extent of PEO modification. Increasing the functionalization (f) of PEO a macroscopic phase separation occurred. To investigate F-HEUR's behavior in homogeneous aqueous solution, sodium dodecyl sulfate (SDS) has been used in concentrations close to the cmc. As reported elsewhere, the addition of a small amount of an anionic surfactant (like SDS) makes easier the solubilization in water of strongly aggregated polymers by formation of mixed micelles involving polymer end groups and surfactant. In this sense SDS stabilizes aqueous solution of HEUR and prevents phase segregation. It was also established that SDS could influence the dynamics of the transient network of APs solutions.[9,20−22]

We have investigated the linear viscoelasticity of solutions (at 25 °C) as a function of F-HEUR concentration (C_{pol}), polymer functionalization f ($f = 0.90$ or 1.0), and the presence (or not) of surfactant. The stress relaxation function $G(t)$ has been measured as a function of temperature and concentration. The main feature is that the stress relaxation function decreases in all experiments performed as a stretched exponential of the form $G(t) = G_0 \exp[-(t/\tau)^{\alpha}]$. Here G_0 denotes the plateau modulus whereas τ is the macroscopic relaxation time of the transient network. Compared with already published data concerning fully hydrogenated end caps,[22,23] τ is found to be about 10^3 times larger and the associated activation energy about twice the one reported in the literature ($40k_BT$ vs $\approx 25k_BT$). These data underline the influence of semifluorinated end groups on the rheological properties and solution behavior of F-HEUR.

2. Experimental Section

2.1. Materials. The F-HEUR polymers are synthesized from PEO of molecular weights 10 000 and 20 000 (Merck). In this study, isophorone diisocyanate (IPDI) (Hüls), sodium dodecyl sulfate salt (SDS), tri-*n*-butyltin hydride, and dibutyltin dilaurate (Aldrich) are used as received without further purification. Perfluorooctyl iodide and 10-undecen-1-ol are provided by ATOFINA. Water for viscometric analysis is distilled and passed through a Milli-Q (Millipore) ion exchange column.

2.2. Synthesis of 11-(Perfluorooctyl)undecan-1-ol. 11-(Perfluorooctyl)undecan-1-ol is prepared in two reaction steps:

(i) A 0.1 mol sample of 10-undecen-1-ol and 0.15 mol of perfluorooctyl iodide were placed in a three-necked round-bottom flask equipped with a reflux condenser, a nitrogen inlet tube, and a magnetic stirrer. The mixture was homogenized by heating to 80 °C, and then 200 mg of azobis(isobutyronitrile) (AIBN) was added. The addition reaction can be followed by ^{19}F NMR.

During the reaction, after 0.5 and 2 h, respectively 100 and 300 mg of AIBN were added. The reaction was monitored (^{19}F NMR) by the decrease of the $-CF_2I$ signal at −64.36 ppm, when the ratio between $-CF_2-CH_2$ and $-CF_2I$ signals remains constant (≈5 h), the reaction is stopped. Completion of the reaction was confirmed by the disappearance (^1H NMR) of the initial double bond signal. Unreacted R_F-I can be eliminated by dissolution in heptane followed by reduced-pressure distillation. 11-(Perfluorooctyl)-10-iodoundecan-1-ol without further purification was reduced by tri-*n*-butyltin hydride.

(ii) A 9.24×10^{-2} mol sample of perfluorooctyl iodo alcohol was reacted with 0.11 mol of tri-*n*-butyltin hydride. 0.01 mol of AIBN dissolved in 30 mL of absolute toluene was added with a siringe via a rubber septum. The solution was stirred for 1 h at 80 °C under nitrogen.

After solvent evaporation by reduced-pressure distillation, the solid obtained was dissolved in a KF-saturated ethylic ether solution, stirred one night, and then filtered and evaporated by reduced-pressure distillation. The solid obtained was purified by recrystallization in *n*-heptane.

Scheme 1. Synthesis of Telechelic Semifluorinated HEUR

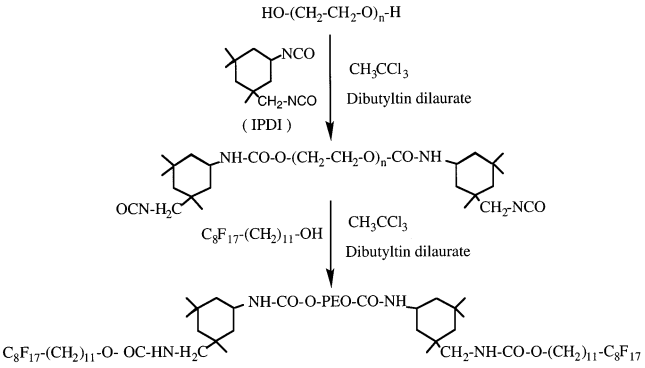

2.3. Synthesis of F_8H_{11}-HEUR. F_8H_{11}-HEUR-20K and F_8H_{11}-HEUR-10K were prepared in two reaction steps (Scheme 1):

(i) Synthesis of Isocyanato Telechelic PEO Prepolymer. In a three-necked 250 mL round-bottom flask, equipped with a nitrogen inlet tube, a condenser with thermometer, and a magnetic stirrer, a 20 g sample of PEO was weighed, and 125 mL of 1,1,1-trichloroethane (CH_3CCl_3) was added. The reaction mixture was nitrogen purged, and water was azeotropically distilled by heating the solvent to reflux (75 °C). A total of 25 mL of solvent was removed to obtain a PEO weight concentration of 20%. (F-HEUR with a functionalization $f = 0.9$ was obtained with a PEO concentration of 10%.) The flask was cooled, the condenser replaced by a Vigreux distillation column, and the reaction mixture nitrogen purged. A very large excess of isophorone diisocyanate (100 equiv of NCO to 1 equiv of OH) and dibutyltin dilaurate (0.15% by mol of IPDI) were added with a syringe. The reaction was stirred for 2 h at 80 °C (50 mn to obtain the F-HEUR-20K90 and 3 h for F-HEUR-10K80).

The warm prepolymer solution filtered before precipitation into petroleum ether was collected on a sintered glass Büchner funnel and dried under reduced pressure. Purification of prepolymer was performed by dissolution in hot CH_3CCl_3 and reprecipitated into petroleum ether. The PEO prepolymer was dried under vacuum at 40 °C for 1 h.

(ii) Synthesis of F_8H_{11}-HEUR. In a three-neck round botton flask as described before, 19 g of isocyanato telechelic PEO prepolymer was dissolved in 100 mL of CH_3CCl_3. The solution was purged with nitrogen, and dibutyltin dilaurate (7.5×10^{-2} mmol, 40 μL) was added. An excess of 11-(perfluorooctyl)-undecan-1-ol (3 equiv of OH to 1 equiv of NCO) dissolved into CH_3CCl_3 (20 mL) was injected into the flask, and the reaction was stirred for 2 h at 80 °C. At this time FT-IR analysis showed the disappearance of the isocyanate band (2250−2300 cm^{-1}). The warm solution was filtered and precipitated into petroleum ether. The F_8H_{11}-HEUR polymers were collected on a Büchner and dried under vacuum at 40 °C for 4 h.

2.4. Characterization of the Thickeners. ^{19}F NMR and ^1H NMR (250 MHz) spectra were recorded on a Bruker AC 250 NMR spectrometer. FT-IR spectra of prepolymers and F-HEUR were recorded on a Bruker IFS 25. At each step of the synthesis, prepolymers and thickeners were analyzed with respect to their molecular weight distribution by size exclusion chromatography (SEC) using a Shimadzu RID-6A differential

refractometer and tetrahydrofuran as the mobile phase (flow rate 1 mL min^{-1}). A set of three PL Gel columns was used with the following pore sizes: 5×10^2, 10^3, and 10^4 Å. A calibration curve was established from poly(ethylene oxide) standards. SEC analysis confirms that the molecular weight distribution of the modified polymer remained unchanged by comparison with the initial product. As a consequence, it could be claimed that polycondensation did not occur in these experimental conditions. The absence of tailing on the elution curve toward low molecular weights side means that the reaction proceeds without noticeable PEO chain degradation.

The degree of functionalization was determined by ^{19}F NMR. The F-HEUR sample (about 50 mg) in $CDCl_3$ solution (0.5 mL) was reacted first with a slight excess (5 μL) of trifluoroacetic anhydride (TFAA) in order to modify residual OH end groups with the formation of trifluoroacetate. ^{19}F NMR resonances of PEO trifluoroacetate end group and TFAA overlap with a chemical shift $\delta = -75.5$ ppm. The separation of the different CF_3 was allowed by esterification of TFAA in excess with 1-butanol (20 μL). The $-CF_3$ resonance of *n*-butyltrifluoroacetate is slightly shifted upfield ($\delta = -75.7$ ppm). The residual OH content was determined by comparison of the relative intensity of signals of PEO trifluoroacetate ($\delta = -75.5$ ppm) and perfluoroalkylated PEO [$\delta(-CF_3) = -81.3$ ppm].

This method of characterization was described with more details in a preceding paper.[8] ^{19}F NMR chemical shifts are given in δ (ppm) upfield from external $CFCl_3$.

Associative polymers considered here have molecular weights closed to 10 000 or 20 000 g mol^{-1}; they differ by the level of chain end modification (f). We will adopt the following nomenclature: F-HEUR-10K80 and F-HEUR-20K90 for the partially modified PEO (f = 80%, 90%) and F-HEUR-20K100 for the fully end-capped PEO (f = 100%).

2.5. Linear Rheology. Dilute solutions were studied using a Ubbelohde capillary viscometer with diameter of 0.56 mm (at constant temperature, $T = 25$ °C). The capillary viscometer was restricted to the investigation of Newtonian solutions.

The static viscosity (η_0) was obtained acccording to

$$\eta_0 = Kt \tag{1}$$

where t is the solution flow time in seconds. The instrument constant K refers to the pure water flow time for which $\eta_0 = 0.8904 \times 10^{-3}$ Pa s^{-1} at 25 °C.

For higher polymer concentrations (typically $C_{pol} > 0.8$ wt %), the F-HEUR telechelic solutions become viscoelastic, and so, a standard rotational rheometer is of appropriate use. The mechanical properties were obtained either on a Rheometrics fluid spectrometer (RFS II) or on a rheometer US200 from Physica, both working either in Couette geometry (gap 1 mm) for viscosity lower than 1 Pa s or in a cone-and-plate geometry (gap 50 μm, angle 0.02 rad) for higher static viscosity η_0.

The linear viscosity was investigated using step-strain experiments, and the stress relaxation function $G(t)$ was determined. In these experiments, a deformation γ_0 is applied to the sample, and the resulting stress $\sigma(t)$ developed in the material is recorded as a function of time. Measurements were carried out for deformation amplitudes $\gamma_0 = 1-30\%$ (linear response) and temperatures ranging between $T = 5$ °C and $T = 40$ °C. The stress relaxation function $G(t)$ is calculated according to

$$G(t) = \sigma(t)/\gamma_0 \tag{2}$$

From the relaxation spectra, the static viscosity can be computed since it equals the integral over time of the $G(t)$ function during the step-strain experiment, i.e.

$$\eta_0 = \int_0^\infty G(t)\, dt \tag{3}$$

3. Experimental Results and Analysis

3.1. Phase Behavior. Fully modified PEO (F-HEUR-20K100) in aqueous medium exhibits a macroscopic phase separation, even at low polymer concentration (C_{pol} = 0.1 wt %). A dilute upper phase, with a low viscosity comparable to that water, coexists with a viscous gel-like condensed lower phase. A similar behavior was reported by Kaczmarski et al.[9] and Pham et al.[24] for C_{16} and C_{18} hydrophobically modified PEO. Phase separation for incompletely end-capped PEO was found to be dependent on PEO molecular weights and extent of modification. F-HEUR 20K90 with $f = 0.9$ leads to homogeneous solutions while F-HEUR-10K80 with a more reduced degree of functionalization ($f = 0.8$) exhibits a phase segregation. No phase separation was mentioned by Xu et al.[17] and by Zhang et al.[25] for HEUR with a semifluorinated end group $C_8F_{17}-(CH_2)_2$. All these results provide evidence that phase separation of HEUR thickeners is dependent on the degree of functinalization, hydrophobic strength of the end group that is reinforced by a perfluorinated segment, and PEO molecular weight. This process is governed by the hydrophobe−hydrophile balance of HEUR and by the extent of end-functionalization.

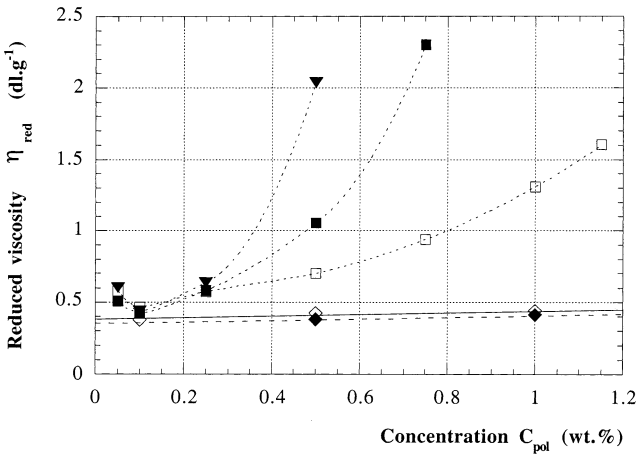

Figure 1. Reduced viscosity from capillary viscometry as a function of polymer concentration C_{pol} in wt % for F-HEUR-20K90 (□), F-HEUR-20K90 in the presence of SDS (■), and F-HEUR-20K100 in the presence of SDS (▼). The reduced viscosities of unmodified PEO-20K alone (◇) and with SDS (◆) are shown for comparison. SDS concentration is 8 mmol L^{-1}. Because of the huge increase of viscosity, capillary viscometry measurements were restricted to low polymer concentrations.

The coexistence of a viscous close-packed phase of micelles and a dilute solution of micelles was proposed by Semenov et al.[26] The attractive energy between flowerlike micelles expected to be large enough (for large aggregation number) and the resulting tendency for micelles to stick together could be significantly reduced by the presence of dangling unmodified PEO chains.

3.2. Viscosity in Dilute Solutions. The reduced viscosity dependence of APs (F-HEUR-10K80 and F-HEUR-20K) on polymer concentration (C_{pol}) is illustrated in Figure 1.

At low concentrations, the reduced viscosity of solutions of F-HEUR-20K90 without SDS varies with concentration C_{pol} according to the Huggins equation:

$$\eta_{red} = [\eta] + k_h[\eta]^2 C_{pol} \tag{4}$$

Fitting the linear portion of experimental data to the Huggins equation determines the intrinsic viscosity [η] and the Huggins coefficient (k_h). The intrinsic viscosity is found very close to that of unmodified PEO-20K

Table 1. Intrinsic Viscosity [η] and Huggins Coefficient k_h of PEO and F-HEUR

	[η] (dL g^{-1})	k_h
PEO-10K	0.25 ± 0.01	0.32 ± 0.01
F-HEUR-10K80 (SDS)	0.26 ± 0.01	8.3 ± 3
PEO-20K	0.38 ± 0.01	0.41 ± 0.03
PEO-20K (SDS)	0.35 ± 0.01	0.45 ± 0.01
F-HEUR-20K90	0.37 ± 0.04	6.8 ± 2
F-HEUR-20K90 (SDS)	0.34[a]	11.2 ± 4[a]

[a] Values mentioned for information only. The limited linear part of the curve does not allow an accurate determination of [η] and k_h.

(Table 1). Similar results were reported by Pham et al.[24] for HEUR-35K end-capped by C_{16} or C_{18} hydrocarbon groups and by Alami et al.[27] for hydrophobically end-capped PEO-20K by C_{12} segment, via an ether linker.

In this range of concentrations 0.08−0.5%, a polymeric chain with two fluorinated hydrophobic tails could not remain free in aqueous solution, and an aggregation of some kind should occur. Small-angle neutron scattering (SANS) has been used to investigate the form and structure factors of F-HEUR-10K and -20K aggregates. It was established that F-HEURs self-assemble into flowerlike micelles, even at low concentration (0.08 wt %).[28,29] Furthermore, the inner core of micelles containing hydrophobic end caps remains unchanged with C_{pol}. From the radius of gyration of F-HEUR-20K80 in D_2O solution (without SDS), determined from SANS experiments[28] ($R_G = 124 \pm 4$ Å), the hydrodynamic radius R_H was estimated ($R_H = 160 \pm 5$ Å) using the relation $R_H^2 = 5R_G^2/3$.

The relationship between the intrinsic viscosity and the hydrodynamic radius

$$[\eta] = \frac{10\pi {R_H}^3 N_A}{3Mp} \tag{5}$$

permits an estimate of the aggregation number $p = 35 \pm 7$ of F-HEUR-20K flowerlike micelles and thus 70 ± 14 semifluorinated groups per micelle. This value for p is in accordance with that established by Séréro[28] ($p = 35 \pm 3$) by SANS from the extrapolated absolute intensity at $q \rightarrow 0$. This value for p is comparable with that estimated by Pham et al.[24] ($p = 33 \pm 9$) for C_{18}-HEUR via eq 5.

The hydrodynamic ratio $g' = [\eta]/[\eta]_{lin}$, where [η] and $[\eta]_{lin}$ are respectively the intrinsic viscosity of star polymer and linear equivalent polymer, calculated from results reported by Grest et al.,[30] leads to $g' = 0.08$. The calculation of the intrinsic viscosity of a linear PEO equivalent to F-HEUR-20K by the Mark−Houwink−Sakurada equation: $[\eta] = KM^a$ with $K = 12.5 \times 10^{-5}$ and $a = 0.78$ leads to $[\eta]_{lin} = 4.53$ dL g^{-1}. The ratio $[\eta]_{F-HEUR-20K}/[\eta]_{linPEO} = 0.08$ provides evidence that the hydrodynamic behavior of F-HEUR-20K is similar to that expected for star-shaped polymers.

The intrinsic viscosity [η] of F-HEUR-20K90 is obtained by extrapolation of η_{red} from solutions in a concentration range where it was clearly established that polymers are associated. A priori the hydrodynamic behavior of end-capped PEO forming flowerlike aggregates should be completely different from that of unmodified PEO chains under nonassociated form. Comparable values of the intrinsic viscosity obtained for these different polymeric species must be considered as fortuitous.

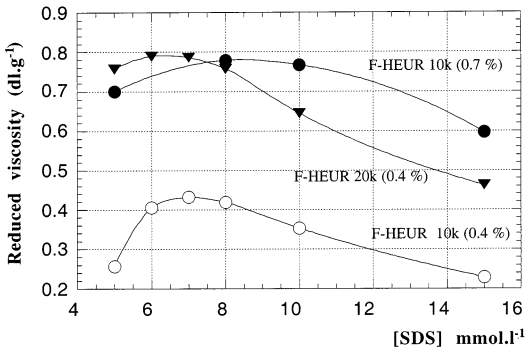

Figure 2. Reduced viscosity of F-HEUR as a function of SDS molar concentration. Between brackets, the polymer concentration in wt %.

The reduced viscosity of F-HEUR solutions is modified by the presence of an anionic surfactant (SDS) (cf. Figure 2). As the amount of surfactant is increased, the reduced viscosity increases, reaches a maximum, and then decreases. These results are consistent with the general assumption that SDS forms mixed aggregates with the hydrophobic stickers, increasing the number of interaggregate connections. The optimum SDS concentration to achieve the highest viscosity appears in the range of the critical micellar concentration (cmc = 8 mmol L^{-1}).

If one considers the molar ratio N = SDS/HEUR, the maximum of viscosity for F-HEUR-20K ($C_{pol} = 0.4$ wt %) is obtained for a value of N ($N \approx 30$), which is twice that for F-HEUR-10K. The SDS aggregation number was reported[31] to be close to 60. If the F-HEUR chains are randomly distributed between SDS micelles, the optimum of viscosity is reached for two F-HEUR-20K chains per SDS micelle. At higher SDS concentrations, the probability of finding several end groups simultaneously, within the same mixed micelle, drops rapidly. In the following results, when SDS will be used in order to obtain homogeneous solutions, the SDS concentration remains constant and equal to the cmc (8 mmol L^{-1}). It is clear that, by this way, the ratio N will be varying inversely with the polymer concentration.

The influence of SDS on the reduced viscosity of F-HEUR can be illustrated by F-HEUR-20K90 behavior as a function of polymer concentration (Figure 1). At low concentrations, up to $C_{pol} = 0.25\%$, η_{red} is not influenced by SDS and the extent of F-HEUR functionalization. With increasing concentration, η_{red} is found to increase drastically in the presence of SDS. For solutions of F-HEUR-20K90 without SDS, the increase of η_{red} is much more moderate. The increase in η_{red} observed in the presence of SDS corresponds to the onset of viscoelasticity of the solutions and reveals the ability of a surfactant to produce a more developed network. A reduction in the number of undesirable unifunctional F-HEUR, with the transformation of dangling end chain to intermicellar link, produces an increase of viscosity.

The Huggins coefficient, k_h, characterizes the interactions of polymer chains with solvent and between themselves. k_h obtained for unmodified PEO-10K ($k_h = 0.32$) and PEO-20K ($k_h = 0.41$) correspond typically to polymer in good solvent. For F-HEUR, the values of k_h ($k_h \geq 6.8$) clearly demonstrate strong polymer chain interactions arising between flowerlike micelles and preceding the onset of a macroscopic network made up of bridged micelles.

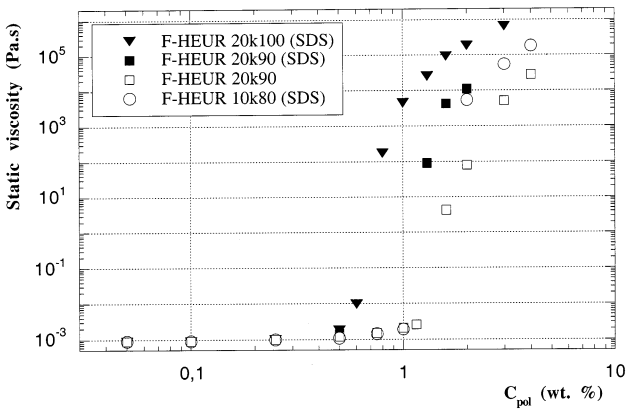

Figure 3. Concentration dependence of the static viscosity (η_0) of F-HEUR in aqueous solution in the presence of SDS (8 mmol L^{-1}) or not (F-HEUR-20K90) at 25 °C. Solutions with low polymer concentration were investigated with the Couette cell in steady shear conditions, while the highest concentrated samples were studied using a cone-and-plate geometry.

3.3. Concentration Dependence on Linear Viscoelasticity. Static viscosities η_0 reported in Figure 3 were obtained from rotational rheometry measurements at $T = 25$ °C. The low C_{pol} aqueous solutions, with low viscosity (typically 1 Pa s), were investigated with a Couette cell in steady shear conditions, while higher concentrated solutions were studied using a cone-and-plate geometry.

Figure 3 shows the effect of F-HEUR concentration on the static viscosity. In the presence of SDS, η_0 starts to rise rapidly at a concentration of the order of 1 wt %. The steep increase in viscosity occurs for fully modified F-HEUR at a lower concentration ($C_{pol} \approx 0.75$ wt %). The divergence of the viscosity, in the vicinity of the threshold concentration denoted C^*_{pol}, indicates the formation of a multiconnected network of mixed micelles. This behavior is interpreted as a sol−viscoelastic transition at C^* between a dilute solution of flowerlike micelles and an infinite cluster of flowers. For partially modified F-HEUR without SDS, the transition occurs over a broader concentration range (1.15−1.6 wt %) and with a more gradual increase of η_0. At relatively low concentration (2 wt %) the different systems exhibit huge viscosities from 10^5 up to 10^8 times that of water. The presence of a perfluorinated end group C_8F_{17} cannot explain by itself such an increase of viscosity.[17] In terms of structural parameters, this effect can be explained by the presence of a long hydrocarbon spacer $(CH_2)_{11}$ that enhances the hydrophobic character of the end group and by the complete extent of chain end modification.

The stress relaxation function $G(t) = \sigma(t)/\gamma_0$, relative to F-HEUR-20K100, obtained in step-strain experiments, is shown in Figure 4 for $C_{pol} = 0.8\%$, 1%, 1.3%, 1.6%, 2%, and 3% ($T = 25$ °C). A double-logarithmic representation has been used to emphasize the huge variation of the stress response. For $C_{pol} \geq 1\%$, $G(t)$ remains almost constant and starts to decrease above 10 s; for $C_{pol} = 0.8\%$, $G(t)$ decreases earlier. Note that the $G(t)$ decrease is fully completed after a given time, which can exceed 1 h ($C_{pol} = 3\%$).

This is a result of great importance; it means that the static viscosity η_0, defined by eq 4, is a finite quantity. The values of η_0 shown in Figure 3 and reported in Table 2 were calculated in this way. From the time-dependent stress relaxation function (Figure 4), it is possible to determine the elastic plateau modulus G_0 by extrapolating $G(t)$ to $t = 0$ and the relaxation time τ of the stress decrease. The time τ can be roughly determined by the relation $G(\tau) = G_0/e$ derived from the Maxwell model. The monoexponential decrease of $G(t)$ according to the Maxwell model was found unsuited to describe the stress relaxation function. A better approximation of the $G(t)$ function was obtained using a stretched exponential:

$$G(t) = G_0 \exp[-(t/\tau)^{\alpha}] \qquad (6)$$

It was clearly established that the relaxation in complex, slowly relaxing, strongly interacting materials often follows the stretched exponential form (6) with $0 < \alpha < 1$. This "anomalous" relaxation appears to be far more common than the "conventional" exponential form

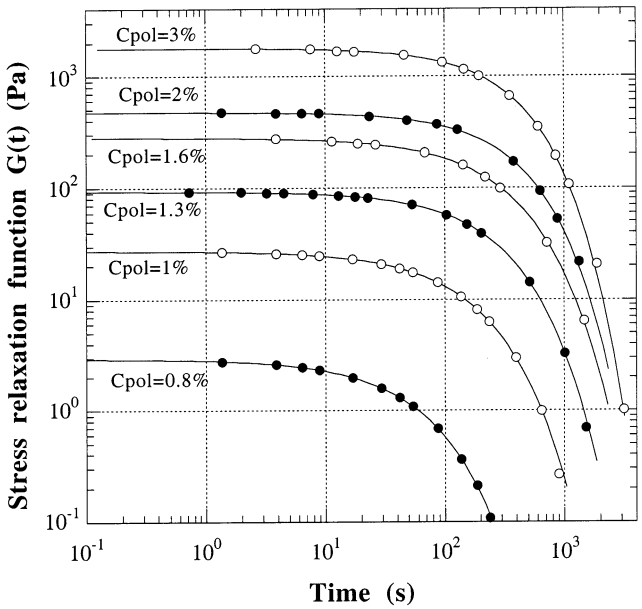

Figure 4. Time dependence of the stress relaxation function $G(t)$ of F-HEUR-20K100 aqueous solutions with SDS (8 mmol L^{-1}) obtained in step-strain experiments for $C_{pol} = 0.8\%$, 1%, 1.3%, 1.6%, 2%, and 3%.

Table 2. Rheological Characteristics of F-HEUR Solutions at 25 °C[a]

F-HEUR	C_{pol} (wt %)	G_0 (Pa)	τ (s)	α	η_0 (Pa s)
10K80 (SDS)	2	38	115	0.71	5390
	3	368.5	141	0.86	55200
	4	1146	148	0.84	186000
20K90	2	5	14	0.82	79
	3	125	38	0.86	5100
	4	500	52	0.86	28320
20K90 (SDS)	1.3	2.7	28	0.71	90
	1.6	62	59	0.80	227
	2	98	105	0.84	11050
20K100 (SDS)	0.7	0.6	24	0.77	16
	0.8	2.9	54	0.78	174
	1	27	147	0.81	4429
	1.3	101	248	0.85	25500
	1.6	293	307	0.88	96240
	2	475	370	0.87	183855
	3	1751	351	0.93	641200

[a] Influence of PEO molecular weight $M_n = 10\,000$ or $20\,000$ g mol^{-1} (10K, 20K), percentage of chain end fonctionnalization (80%, 90%, 100%), and surfactant (SDS). SDS is added at a concentration of 8 mmol L^{-1}. G_0 is the elastic plateau modulus. τ is the relaxation time of the stress decrease. α is the exponent of the stretched exponential (eq 7). η_0 is the static viscosity obtained from the $G(t)$ integration (eq 4).

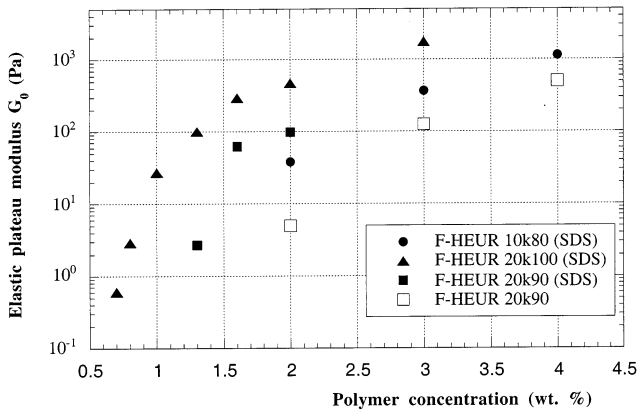

Figure 5. Polymer concentration (C_{pol}) dependence of the elastic plateau modulus (G_0) for different F-HEUR systems at 25 °C in the presence of SDS (filled symbols) or not (open symbols).

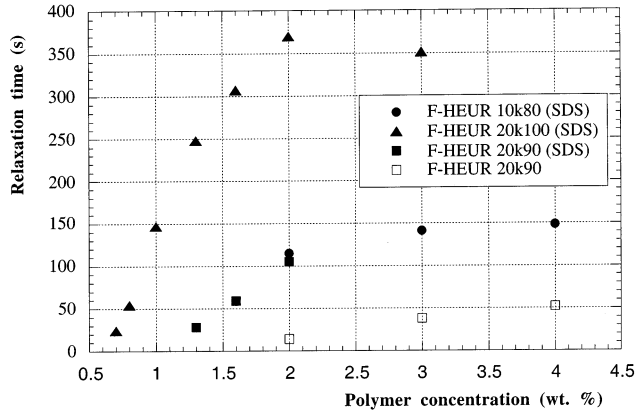

Figure 6. Effect of polymer concentration (C_{pol}) on the relaxation time (τ) for aqueous solutions of F-HEUR at 25 °C in the presence of SDS (SDS) or not.

($\alpha = 1$).[32] The solid line through the data points in Figure 4 proceeds from best fit calculations according to eq 6. As can be seen, experimental data are in excellent agreement with a stretched exponential to describe the $G(t)$ function. The three fitting constants G_0, τ, and α are listed in Table 2 for three different fluorinated end-capped PEO: F-HEUR-10K80, F-HEUR-20K90, and F-HEUR-20K100, in the presence or not of surfactant (SDS). Whatever the system HEUR/water/(SDS), for increased polymer concentrations, both G_0 and τ are enhanced. The increase of the exponent α according to C_{pol} is less pronounced; α was found ranging from 0.71 up to 0.93. The logarithmic plot of G_0 vs C_{pol} (cf. Figure 5) has been used to underline the large increase of the elastic plateau modulus in relation with the presence of SDS and the extent of PEO chain end functionalization. For all the systems studied, the relaxation times of F-HEUR were found higher than 1 s, even at low polymer concentration. The influence of C_{pol} on τ is shown in Figure 6. In presence of SDS, a huge increase of τ is observed, with unusual values ranging between 100 and 400 s. For F-HEUR-20K90, at $C_{pol} = 2$ wt %, the values of τ differ by a factor 7.5 due to the presence or not of SDS. The relaxation time is also enhanced by the level of PEO chain end modification.

3.4. Temperature Dependence on Linear Viscosity. The effect of temperature on the viscoelastic response of F-HEUR-10K80 solutions in the presence of SDS (8 mmol L^{-1}) has been investigated at different concentrations, $C_{pol} = 2$, 3, and 4 wt %. The adjustable parameters G_0, τ, α, and η_0 obtained from the analysis of the stress relaxation function $G(t)$ (eq 6) are listed in Table 3. Step-strain experiments were performed for temperatures ranging from 5 up to 40 °C. At low temperature ($T = 5$ °C) a huge value of τ, exceeding 25 mn, is observed. When a deformation is applied, the time necessary for the system to recover the equilibrium with an undeformed state exceeds 2 h. Increasing temperature the relaxation time (τ) drops to few seconds at 40 °C.

With the rise of temperature, a decrease of G_0, τ, and η_0 was observed. Similar effects of temperature on rheological parameters were obtained for the F-HEUR-20K90 solutions (Table 4). The variation of these parameters was enhanced by the addition of SDS surfactant in the aqueous HEUR solution. At the same polymer concentration ($C_{pol} = 2$ wt %) and temperature higher values of G_0, τ, α, and η_0 were obtained for F-HEUR-20K100 in the presence of SDS (cf. Table 5).

The temperature dependence of relaxation time and static viscosity is shown in Arrhenius form in Figure 7 for F-HEUR-10K80 at different concentrations and for F-HEUR-20K at $C_{pol} = 2$ wt % in Figure 8. Both the relaxation time and viscosity present an Arrhenius law temperature dependence. The data obtained from the relaxation time variation was found to give a mean value for the activation energy (E_a) of 117.4 kJ mol^{-1}, whereas a mean value of 143.4 kJ mol^{-1} was found from

Table 3. Influence of Temperature on the Viscoelastic Parameters of Solutions of F-HEUR-10K80 in Presence of SDS (8 mmol L^{-1}) at Different Concentrations[a]

C_{pol} (wt %)	T (°C)	G_0 (Pa)	τ (s)	α	η_0 (Pa s)
2	5	59	1537	0.84	99030
	10	72	832	0.85	65180
	15	60	446	0.82	23660
	20	39	190	0.82	8330
	25	38	115	0.71	5390
	30	33	50	0.65	2180
	35	19	13.5	0.59	384
	40	15	6	0.57	149
3	20	444	313	0.85	149800
	25	368.5	141	0.86	55200
	30	286.5	65	0.83	20500
	35	249	29	0.82	7890
	40	226	13	0.80	3160
4	25	1146	148	0.84	186010
	27.5	1043	101	0.84	114400
	30	961	69	0.83	71360
	35	873	34	0.85	31495
	40	813	16	0.84	13160

[a] Results obtained from the analysis of the stress relaxation function $G(t)$ in terms of stretched exponential (eq 7).

Table 4. Influence of Temperature on the Viscoelastic Parameters[a] of Solutions of F-HEUR-20K90 at Polymer Concentration $C_{pol} = 2$ wt % and Influence of SDS on the Rheological Behavior (SDS Concentration 8 mmol L^{-1})

surfactant	T (°C)	G_0 (Pa)	τ (s)	α	η_0 (Pa s)
no	15	8.5	61	0.83	580
	20	5.7	28	0.83	180
	25	5.3	14	0.81	83
SDS	20	214	120	0.83	28390
	25	123	104	0.82	13970
	30	105	70	0.83	7690
	35	75	26	0.80	1890

[a] Definitions are identical to those of Table 2.

Table 5. Influence of Temperature on the Viscoelastic Parameters of Solutions of F-HEUR-20K100 in Presence of SDS (8 mmol L^{-1}) and Influence of Polymer Concentration (C_{pol})[a]

C_{pol} (wt %)	T (° C)	G_0 (Pa)	τ (s)	α	η_0 (Pa s)
0.8	15	8.3	445	0.83	23660
	25	2.9	54	0.79	5390
	35	0.3	2.2	0.67	384
2	20	435	751	0.79	377000
	25	472	393	0.86	200000
	30	453	193	0.86	95100
	35	212	61	0.79	15110
	40	157	29	0.80	5100

[a] Results obtained from the analysis of the stress relaxation function $G(t)$ in terms of stretched exponential (eq 7). Definitions are identical to those of Table 2.

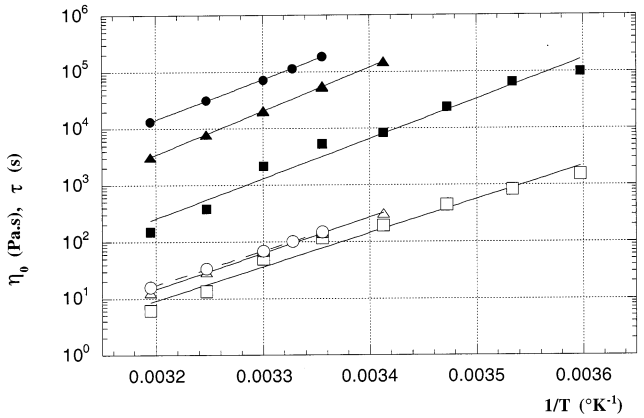

Figure 7. Arrhenius plots of static viscosity η_0 and relaxation time τ obtained from best fit calculations of the stress relaxation $G(t)$ (eq 7) for F-HEUR 10K80 at different concentrations: C_{pol} = 2 wt % (□), 3 wt % (△), and 4 wt % (○); open symbols are used for the relaxation time and filled ones for the static viscosity.

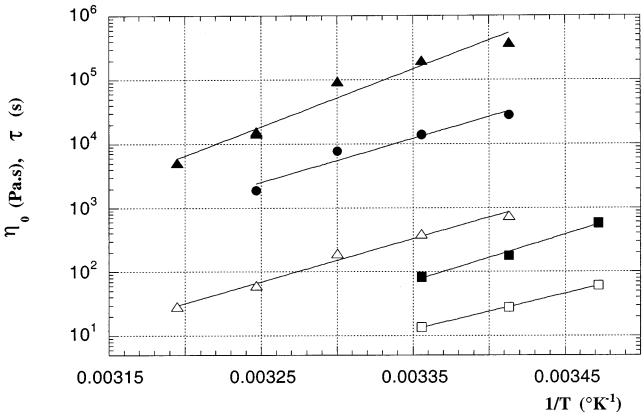

Figure 8. Arrhenius plots of static viscosity η_0 and relaxation time τ obtained from best fit calculations of the stress relaxation $G(t)$ (eq 7) for different F-HEURs: 20K100 (△) and 20K90 in the presence of SDS (○) or not (□) at 2 wt % (open symbols are used for the relaxation time and filled ones for the static viscosity).

viscosity data. The values of the activation energy for the different F-HEUR systems are listed in Table 6.

4. Discussion

The aim of the present paper is to correlate the unusual rheological properties of fluorinated end-capped PEO with structural parameters of the different F-HEUR systems.

Table 6. Activation Energy (E_a) for Different F-HEUR Systems Obtained from Fit Calculation of Arrhenius Plot of Relaxation Time and Viscosity

F-HEUR	C_{pol} (wt %)	E_a(from τ data) (kJ mol^{-1})	E_a (from η data) (kJ mol^{-1})
10K80 (SDS)	2	113.9	135.1
	3	121.2	147.5
	4	115.4	135.7
20K90	2	107.5	139.2
20K90 (SDS)	2	*a*	130.6
20K100 (SDS)	2	128.8	172.2

[a] This set of data could not be fitted correctly due to its limited extent.

The macroscopic phase separation observed for some F-HEUR, even at low polymer concentration (C_{pol} < 1 wt %), was found to be dependent on the chemical structure of PEO chain end. The sol−gel coexistence is very sensitive to chain end functionalization. A 10% uncompletely end-capped F-HEUR-20K did not phase separate. François et al.[33] reported the phase segregation of hydrocarbon end-capped PEO when the balance hydrophobic/hydrophilic exceeded a critical value. Typically, this critical value is obtained for $C_{18}H_{37}$−HEUR-20K. The phase separation observed for F-HEURs is revealing the strong hydrophobicity of the semifluorinated C_8F_{17}−$(CH_2)_{11}$ end group. PEO-20K terminated by fluoroalkyl groups [C_8F_{17}−$(CH_2)_2$− or $C_{10}F_{21}$−$(CH_2)_2$−] were recently reported as non-phase-separating systems.[34] That clearly point out the influence of the hydrocarbon spacer −$(CH_2)_{11}$− on phase behavior. In our first report on F-HEUR-10K,[18] the phase separation was not detected. That could be explained by the uncomplete chain end functionalization (the degree of substitution was not determined) and by polycondensation leading to telechelic PEO chains with twice (or even more) the initial hydrophilic chain length.

The form and structure factors of F-HEUR aggregates have been investigated by small-angle neutron scattering.[18,29] The aggregation number "p" of the flowerlike micelles was estimated to p = 49 ±6 for F-HEUR-10K and p = 35 ± 3 for F-HEUR-20K. The cores of the flowers are built up by 2p hydrophobic end groups. The phase segregation observed for F-HEUR confirms the theoretical predictions of Semenov et al.[26] These authors demonstrated that the attractive energy between flowers was large for large aggregation numbers "p". So that the micelles have a tendency to stick together and phase separate into two phases. The gel phase can be considered as a micellar phase where the micelles are connected by bridges in a reversible process. The polymer concentration in the micellar phase (phase of close-packed micelles) is of order of C^*, the overlapping concentration of flowers. According to Semenov,[26] the debridging time (characteristic time of transformation of a bridge to a loop) is expected to be very long.

The solubilization of F-HEUR-10K80 and F-HEUR-20K100 was achieved by addition of an anionic surfactant (SDS) at a concentration of 8 mmol L^{-1}, close to the cmc. In these conditions, the surfactant could be incorporated into the core of the flowers and/or self-assemble into independent micelles. The influence of SDS on rheological parameters can be clearly emphasized only with the F-HEUR-20K90. At low polymer concentration (typically C_{pol} < 1 wt %) the static viscosity of F-HEUR solutions is found to be weakly influenced by SDS. The onset of viscoelasticity of the solutions, corresponding to the overlapping concentra-

tion C^* ($C^* \sim 1.5$ wt %), seems to appear at slightly lower concentration in the presence of SDS (cf. Figure 3). At $C_{pol} = 2$ wt %, the value of the elastic plateau modulus G_0 is increased by a factor 20 due to the presence of SDS. G_0 characterizes the degree of entanglement of the network; it is in linear relation with the density of elastically active chains bridging aggregates. At this polymer concentration ($C_{pol} = 2$ wt %) the relaxation time τ increases in the presence of SDS. These results are consistent with the formation of mixed aggregates in which SDS molecules are incorporated into the core of the flowerlike micelles.

Annable et al.[23] have ascribed the process dominating the relaxation time τ to the disengagement of the hydrophobic end group from the flowerlike micelle. τ corresponding to the lifetime of the micellar junction is governed by the energy barrier associated with the disengagement of one semifluorinated end group from the core of a micelle. Because of the presence of the SDS anionic head in the vicinity of the micelle core, the expulsion of the fluorinated end group requires the crossing of a higher potential barrier.

The unusual relaxation times ($\tau > 100$ s) observed for F-HEUR systems (cf. Table 2) are enhanced by the presence of SDS. The relaxation times reported by Xu et al.[17] for fluorinated [$C_8F_{17}-(CH_2)_2$] HEUR-35K range from 2 to 100 ms according to the polymer concentrations. These long relaxation times observed for F-HEURs are associated with high activation energies deduced from η_0 ($1/T$) and τ ($1/T$) Arrhenius plots. This is in agreement with the transient network theory proposed by Tanaka and Edwards.[35] These authors state that the disengagement rate of a chain from a junction can be described by an expression of the form $\tau^{-1} = w_0 \exp(-E_a/kT)$, where ω_0 is a characteristic frequency of thermal vibration and E_a is the potential barrier to the exit of a chain end from a junction. For a nonfluorinated $C_{20}-$HEUR, Ng et al.[36] reported a value of the activation energy of about 107 kJ mol^{-1}.

The huge increase in the static viscosity η_0 at concentrations beyond C^* can be attributed to the existence of very long relaxation times. According to the theory of rubber elasticity extended to transient networks, the magnitude of the plateau modulus G_0 can be related to the number density of elastically active chains ν_0 by the relation $G_0 = \nu_0 k_B T$. The proportion of mechanically active chains between hydrophobic clusters can be estimated by the relation[17,22,36] $\nu_0/n = G_0/nk_BT$. At the onset of viscoelasticity, at a concentration of the order of 1 wt %, low values of ν_0/n are obtained (2.2×10^{-2}) for the F-HEUR-20K100 system. That implies that only one chain over 45 acts as a connecting cross-link between aggregates. In Figure 9, one can observe an increase of elastically active junctions (ν_0/n) with the augmentation of polymer concentration. It seems therefore that the topology of the network is changing as it is diluted. The effect of dangling chains due to uncomplete chain end modification can be pointed out. A reduction in both the density of elastically active chain and the static viscosity is observed when the temperature is increased (cf. Figure 10). This means that some of the active bridging chains disengage more easily from the micellar junction as the temperature increases.

From time response in step-strain experiments it was shown that the stress relaxation modulus of F-HEUR systems could not be correctly fitted by a single-exponential function.[18] The $G(t)$ function is best fitted

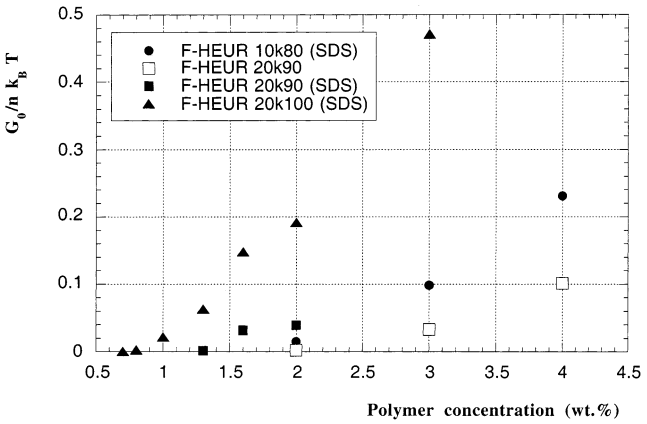

Figure 9. Fraction of elastically active chains (G_0/nk_BT) as a function of polymer concentration for different F-HEURs. Filled and open symbols referred respectively to solutions in the presence of SDS ([SDS] = 8 mmol L^{-1}) and without SDS ($T = 298$ K).

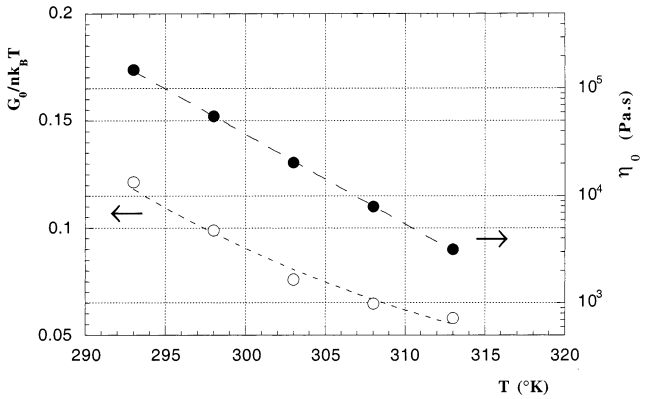

Figure 10. Plot of fraction of elastically active chains (○) and static viscosity η_0 (●) vs temperature for 3.0 wt % aqueous solutions of F-HEUR-10K80.

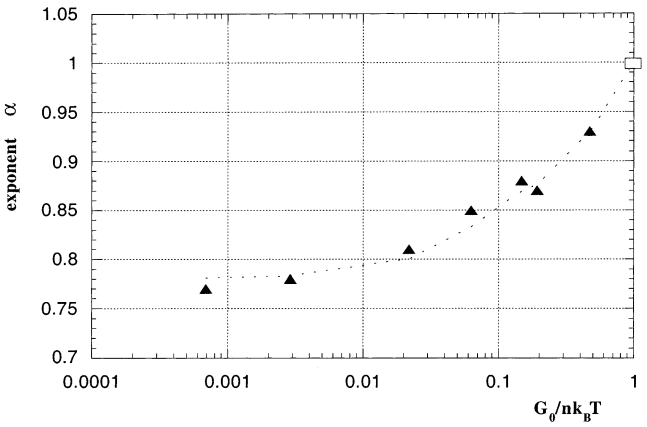

Figure 11. Variation of the exponent α (eq 7) as a function of the fraction of elastically active chains (G_0/nk_BT) for aqueous solutions of F-HEUR-20K100 (SDS) ($T = 25$ °C).

by a stretched exponential (cf. eq 7). The exponent α is a crucial parameter; it has been found varying from 0.57 up to 0.93 according to C_{pol} and temperature for the different F-HEUR systems (cf. Tables 2 and 3). For the F-HEUR-20K100 system, the exponent α was plotted (Figure 11) vs the fraction of elastically active chains, according to polymer concentration. The extrapolation of the curve $\alpha = f(\eta_0/n)$ to $\eta_0/n = 1$ leads to $\alpha = 1$. Thus, increasing polymer concentration C_{pol}, the fraction of bridging chains increases and the F-HEUR solutions

evolve from complex, a slowly relaxing and strongly interacting system toward pure Maxwellian behavior, characterized by a single relaxation process. It seems therefore that the topology of the transient network is changing with the polymer concentration. At concentrations lower than the onset of viscoelasticity or slightly higher than C^*, the F-HEUR system exhibits a complex behavior with probably different relaxation behavior.

5. Conclusions

We have synthesized fluorinated hydrophobically modified ethoxylated urethanes (F-HEUR) with a well-defined structure. The phase segregation with a dilute upper phase that coexists with a viscous gel-like lower phase was found depending on the hydrophobic/hydrophilic balance (PEO chain length) and degree of chain end modification.

The steep increase of the static viscosity at F-HEUR concentrations of about 1 wt %, corresponding to the sol−viscoelastic transition, is enhanced by the presence of surfactant (SDS) and by the degree of functionalization. The divergence of viscosity, in the viscinity of the threshold concentration C^*, is interpreted by the formation of a multiconnected network of flowerlike aggregates. From capillary viscometry results, obtained at low-concentrated solutions, the aggregation number was estimated to 35 ± 7 for the F-HEUR-20K system. The huge increase of the static viscosity η_0 is consistent with the variation of the elastic plateau modulus G_0 and relaxation time τ. The main relaxation process in these end-capped systems is the disengagement of the hydrophobic end group from the cluster. The perfluorinated end group C_8F_{17} reinforces the hydrophobic character of the end caps. As a consequence, the lifetime of the fluorinated end group in the cluster is much more important than for hydrocarbon derivatives. Because of the presence of the perfluorinated end group, the activation energy that represents the energy potential barrier required for the disengagement of the fluorinated segment is increased. The stress relaxation function $G(t)$ cannot be correctly fitted using the Maxwell model. The exponent α of the stretched exponential (eq 7) increases and tends toward 1 with the augmentation of polymer concentration and density of elastically active chains (G_0/nk_BT). The presence of the perfluorinated end groups leads to rheological behavior unusual with nonfluorinated associative polymers.

Acknowledgment. We are grateful to ATOFINA for providing the perfluoroiodoalkane and undecanol used as starting compounds for this research.

References and Notes

(1) Winnik, M. A.; Yekta, A. *Curr. Opin. Colloid Interface Sci.* **1997**, *2*, 424.
(2) Knoef, A. J. M.; Slingerland, H. *JOCCA* **1992**, *9*, 335.
(3) Landoll, L. M. *J. Polym. Sci., Polym. Chem. Ed.* **1982**, *20*, 443.
(4) Hwang, F. S.; Hogen-Esch, T. E. *Macromolecules* **1993**, *26*, 3156.
(5) Xie, X.; Hogen-Esch, T. E. *Macromolecules* **1996**, *29*, 1734.
(6) Abrahmsen-Alami, S.; Stilbs, P. *J. Phys. Chem.* **1994**, *98*, 6359.
(7) Su, Z.; Wu, D.; Ling Hsu, S.; McCarthy, T. J. *ACS Polym. Prepr.* **1997**, *38*, 951.
(8) Hartmann, P.; Collet, A.; Viguier, M. *J. Fluorine Chem.* **1999**, *95*, 145.
(9) Kaczmarski, J. P.; Glass, J. E. *Macromolecules* **1993**, *26*, 5149.
(10) Alami, E.; Abrahmsen-Alami, S.; Vasilescu, M.; Almgren, M. *J. Colloid Interface Sci.* **1997**, *193*, 152.
(11) Lundberg, D. J.; Brown, R. G.; Glass, J. E.; Eley, R. R. *Langmuir* **1994**, *10*, 3027.
(12) Annable, T.; Ettelaie, R. *Macromolecules* **1994**, *27*, 5616.
(13) Kaczmarski, J. P.; Glass, J. E. *Langmuir* **1994**, *10*, 3035.
(14) Yekta, A.; Xu, B.; Duhamel, J.; Adiwidjaja, H.; Winnik, M. A. *Macromolecules* **1995**, *28*, 956.
(15) May, R.; Kaczmarski, J. P.; Glass, J. E. *Macromolecules* **1996**, *29*, 4745.
(16) Zhang, K.; Hogen-Esch, T. E.; Boschet, F.; Margaillian, A. *ACS Polym. Prepr.* **1996**, *37*, 731.
(17) Xu, B.; Li, L.; Yekta, A.; Masouni, Z.; Kanagalingam, S.; Winnik, M. A.; Zhang, K. Macdonald, P. M. *Langmuir* **1997**, *13*, 2447.
(18) Cathebras, N.; Collet, A.; Viguier, M.; Berret, J. F. *Macromolecules* **1998**, *31*, 1305.
(19) Zhang, H.; Pan, J.; Hogen-Esch, T. E. *Macromolecules* **1998**, *31*, 2815.
(20) Zhang, K.; Xu, B.; Winnik, M. A.; Macdonald, P. M. *J. Phys. Chem.* **1996**, *100*, 9834.
(21) Binana-Limbele, W.; Clouet, F.; François, J. *J. Colloid Polym. Sci.* **1993**, *271*, 748.
(22) Annable, T.; Buscall, R.; Ettelaie, R.; Shepherd, P.; Wittlestone, D. *Langmuir* **1994**, *10*, 1060.
(23) Annable, T.; Buscall, R.; Ettelaie, R.; Wittlestone, D. *J. Rheol.* **1993**, *37*, 695.
(24) Pham, Q. T.; Russel, W. B.; Thibeault, J. C.; Lau, W. *Macromolecules* **1999**, *32*, 2996.
(25) Zhang, H.; Hogen-Esch, T. E. *Langmuir* **1998**, *14*, 4972.
(26) Semenov, A. N.; Joanny, J. F.; Khokhlov, A. R. *Macromolecules* **1995**, *28*, 1066.
(27) Alami, E.; Almgren, M.; Brown, W. *Macromolecules* **1996**, *29*, 2229.
(28) Séréro, Y. Thèse de Doctorat, Université de Montpellier II, 1999, unpublished.
(29) Séréro, Y.; Aznar, R.; Berret, J. F.; Calvet, D.; Collet, A.; Viguier, M. *Phys. Rev. Lett.* **1998**, *81*, 5584.
(30) Grest, G. S.; Fetters, L. J.; Huang, J. S.; Dieter, R. *Adv. Chem. Phys.* **1996**, *44*, 67.
(31) Kratohvil, J. P. *J. Colloid Interface Sci.* **1980**, *75*, 271.
(32) Palmer, R. G.; Stein, D. L.; Abrahams, E.; Anderson, P. W. *Phys. Rev. Lett.* **1984**, *53*, 958.
(33) François, J.; Maître, S.; Rawiso, M.; Sarazin, D.; Beinert, G.; Isel, F. *Colloids Surf. A: Phys. Eng. Aspects* **1996**, *112*, 251.
(34) Kornfield, J. A.; Tae, G.; Hubbell, J. A.; Johannsmann, D. *Proc. XIIIth Int. Congress Rheol. Cambridge UK* **2000**, 1−402.
(35) Tanaka, F.; Edwards, S. F. *J. Non-Newtonian Fluid Mech.* **1992**, *43*, 247.
(36) Ng, W. K.; Tam, K. C.; Jenkins, R. D. *J. Rheol.* **2000**, *44*, 137.

MA011729A